arXiv:1410.3803v1 [cond-mat.mes-hall] 14 Oct 2014

Engineering semiconductor hybrids for sensing

Godfrey Gumbs[1,2], Andrii Iurov[1] and Danhong Huang[3]

[1]*Department of Physics and Astronomy,*

Hunter College of the City University of New York,

695 Park Avenue, New York, NY 10065, USA

[2] *Donostia International Physics Center (DIPC),*

P de Manuel Lardizabal, 4, 20018 San Sebastian, Basque Country, Spain

[3]*Air Force Research Laboratory, Space Vehicles Directorate,*

Kirtland Air Force Base, NM 87117, USA

(Dated: October 15, 2014)

Abstract

The effect of screening of the coulomb interaction between two layers of two-dimensional electrons, such as in graphene, by a highly doped semiconducting substrate is investigated. We employ the random-phase approximation to calculate the dispersion equation of this hybrid structure in order to determine the plasmon excitation spectrum. When an electric current is passed through a layer, the low-frequency plasmons in the layer may bifurcate into separate streams due to the current-driving effect. At a critical wave vector, determined by the separation between layers and their distance from the surface, their phase velocities may be in opposite directions and a surface plasmon instability leads to the emission of radiation. Applications to detectors and other electromagnetic devices exploiting nano-plasmonics are discussed.

PACS numbers: 73.21.-b, 71.70.Ej, 73.20.Mf, 71.45.Gm, 71.10.Ca, 81.05.Ue

I. INTRODUCTION AND FORMALISM

Rapid progress has been made in recent years in combining two or more different types of materials to form hybrid nanoparticles on the same nanosystem [1–10]. The main goal of these endeavors is to produce unusual materials with desired functionality such as sensors. Examples include inorganic cage structures obtained by a selective edge growth mechanism of the metal onto the semiconductor nanocrystal. Successful approaches now exist for synthesizing composites with a high degree of control over their shapes, compositions and interfacial properties. The advances in architecture are very impressive and the resulting advanced materials are now being investigated for application of hybrid nanoparticles in electronic devices such as a microlaser, optical components, catalysis, and photocatalysis. A necessary condition for efficient operation of these composite structures is electronic coupling across the constituent interfaces.

This paper focuses on a doped two-dimensional (2D) semiconductor layer hybrid nanoparticle structure for which there is a high degree of control over its performance as a source of electromagnetc radiation. We point out some challenges for further understanding and development of semiconductor-metal hybrid nanoparticles. Specifically, we consider a composite nano-system as shown in Fig.[1] consisting of a thick layer of conducting substrate on whose surface the plasmon is activated in proximity with a pair of thin layers. We demonstrate how the screening of the Coulomb coupling of the plasmons in this pair of layers by the charge density fluctuations on the surface of a semi-infinite substrate affects the surface plasmon instability that leads to the emission of radiation (spiler). The excitation of these plasmon modes is induced by resonant external optical fields. As an emitter, the spiler may be activated optically. Spiler exploits the flexibility of choosing its constituents to produce coherent sources of radiation. Applications to photodetectors and electromagnetic-wave devices exploiting nano-plasmonics are explored.

Our approach models an ensemble consisting of a pair of 2D layers and a thick layer of a conducting medium that emits radiation when an electric field splits the plasmon spectrum which results in an instability as the phase velocities associated with these plasmon branches have opposing signs at a common frequency.

In our formalism, we consider a nano-scale system consisting of a pair of 2D layer structure

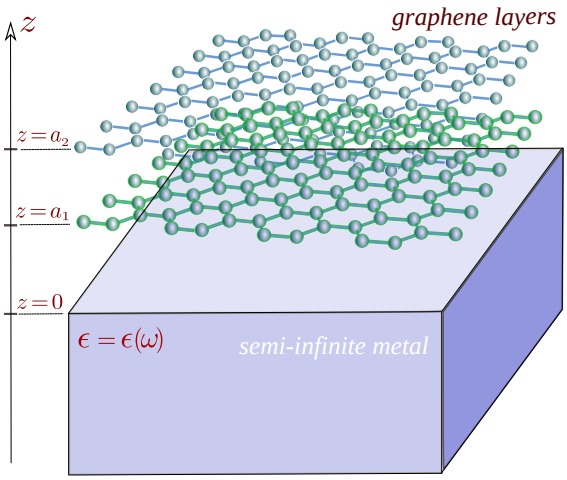

FIG. 1: (Color online) Schematic illustration of a spiler generator consisting of a thick (semi-infinite) conducting material on whose surface a plasmon resonance may induce an instability by coupling to the 2D plasmons on a pair of thin layers such as graphene, silicene or 2DEG at a hetero-interface.

with a double layer positioned at $z = a_1$ and $z = a_2$ $(0 < a_1 < a_2)$ and a thick conducting material. The layer may be monolayer graphene or a 2D electron gas (2DEG), such as a semiconductor inversion layer or a high electron mobility transistor. The graphene layer may have a gap, thereby extending the flexibility of the composite system that also incorporates a thick layer of conducting material as depicted in Fig. 1. The excitation spectra of allowable modes will be determined from the solutions of the dispersion equation which includes the screened Coulomb coupling between layers and between each layer and the semi-infinite substrate. Following standard procedures within the random-phase approximation (RPA) [11,12], calculation shows that the plasmon dispersion equation is $S_C^{(2)}(q_{||},\omega) = 0$, where

$$
\begin{aligned}
S_c^{(2)}(q_{||},\omega) &= \left\{1 + \frac{2\pi e^2}{\epsilon_s q_{||}}\,\Pi_{2D;2}^{(0)}(q_{||},\omega)\left[1 + e^{-2q_{||}a_2}\,\frac{\omega_p^2}{2\omega^2-\omega_p^2}\right]\right\} \\
\times &\left\{1 + \frac{2\pi e^2}{\epsilon_s q_{||}}\,\Pi_{2D;1}^{(0)}(q_{||},\omega)\left[1 + e^{-2q_{||}a_1}\,\frac{\omega_p^2}{2\omega^2-\omega_p^2}\right]\right\} \\
- &\left(\frac{2\pi e^2}{\epsilon_s q_{||}}\right)^2 \Pi_{2D;1}^{(0)}(q_{||},\omega)\,\Pi_{2D;2}^{(0)}(q_{||},\omega)\left[e^{-q_{||}|a_1-a_2|} + e^{-q_{||}(a_1+a_2)}\,\frac{\omega_p^2}{2\omega^2-\omega_p^2}\right]^2 ,
\end{aligned}
\tag{1}
$$

whose $\Pi_{2D}^{(0)}(q_{||},\omega)$ is the 2D polarization function and ω_p is the bulk plasma frequency of the semi-infinite medium. In our numerical calculations, we employ $\Pi_{2D}^{(0)}(q_{||},\omega) \approx Cq_{||}^2/\omega^2$. For

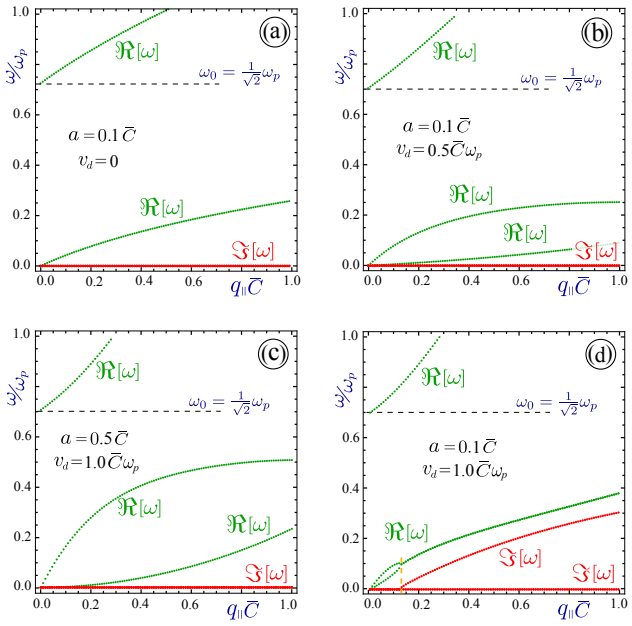

FIG. 2: (Color online) Complex frequencies yielding the plasmon dispersion (real part) and inverse lifetime (imaginary part) for a 2D layer and a semi-infinite dielectric medium as presented in Fig. 1. Panel (a) demonstrates the case when there is no drift current, whereas panels (b), (c) and (d) display the situations with a finite drift velocities $v_d = 0.5\,\bar{C}\omega_p$, $1.0\,\bar{C}\omega_p$ and $1.0\,\bar{C}\omega_p$. Panel (c) corresponds to $a = 0.5\,\bar{C}$ for the distance between the layer and the surface, while the three other panels (a), (b) and (d) to $a = 0.1\,\bar{C}$.

a 2DEG, we have $C = n_{2D}/m^*_{2D}$ with electron density n_{2D} and electron effective mass m^*. For graphene, we find

$$C = \frac{2\mu}{\pi\hbar^2}\left\{1 - \frac{\Delta^2}{\mu^2}\right\} \ , \tag{2}$$

where μ is the chemical potential and Δ is the induced gap between valence and conduction bands. Then, we obtain a quartic equation in ω^2. The plasmon frequencies in this approximation are

$$\begin{aligned}
\Omega_1(q_\parallel)/\omega_p &= 1/\sqrt{2} + q_\parallel\,(\overline{C}_1 + \overline{C}_2)/\sqrt{2} + \mathcal{O}[q_\parallel^2] \ , \\
\Omega_2(q_\parallel)/\omega_p &= q_\parallel\sqrt{\overline{C}_1 a_1 + \overline{C}_2 a_2 + \sqrt{\mathcal{A}}} + \mathcal{O}[q_\parallel^2] \ , \\
\Omega_3(q_\parallel)/\omega_p &= q_\parallel\sqrt{\overline{C}_1 a_1 + \overline{C}_2 a_2 - \sqrt{\mathcal{A}}} + \mathcal{O}[q_\parallel^2] \ ,
\end{aligned} \tag{3}$$

where $\mathcal{A} \equiv (\overline{C}_1 a_1 - \overline{C}_2 a_2)^2 + 4\overline{C}_1\overline{C}_2 a_1^2$. Here, in our notation, $\overline{C}_j = 2\pi e^2 C_j/(\epsilon_s\omega_p^2)$ for

$j = 1, 2$. The spectral function yields real frequencies. A 2D layer interacting with the half-space has two resonant modes. Each pair of 2D layers interacting in isolation far from the half-space conducting medium supports a symmetric and an antisymmetric mode [13]. In the absence of a driving current, the analytic solutions for the plasmon modes for a pair of 2D layers that are Coulomb coupled to a half-space are given by the term $4\overline{C}_1\overline{C}_2a_1^2$ which plays the role of "Rabi coupling". Clearly, for long wavelengths, only $\Omega_1(q_\parallel)$ depends on ω_p. However, the excitation spectrum changes dramatically when a current is driven through the configuration. Under a constant electric field, the carrier distribution is modified, as may be obtained by employing the relaxation time approximation in the equation of motion for the center-of-mass momentum. For carriers in a parabolic energy band with effective mass m^* and drift velocity $\mathbf{v}_d$ determined by the electron mobility and the external electric field, the electrons in the medium are redistributed. This is determined by a momentum shift in the electron wave vector $\mathbf{k}_\parallel \to \mathbf{k}_\parallel - m^*\mathbf{v}_d/\hbar$ in the thermal-equilibrium Fermi function $f_0(\epsilon_\mathbf{k})$. By making a change of variables in the well-known Lindhard polarization function $\Pi_{2D}^{(0)}(q_\parallel, \omega)$, this effect is equivalent to a frequency shift $\omega \to \omega - \mathbf{q}_\parallel \cdot \mathbf{v}_d$. For massless Dirac fermions in graphene with linear energy dispersion, this Doppler shift in frequency is not in general valid for arbitrary wave vector. This is our conclusion after we relate the surface current density to the center-of-mass wave vector in a steady state. Our calculation shows that the redistribution of electrons leads to a shift in the wave vector appearing in the Fermi function by the center-of-mass wave vector $\mathbf{K}_0 = (k_F/v_F)\mathbf{v}_d$ where k_F and v_F are the Fermi wave vector and velocity, respectively. However, in the long wavelength limit, $q_\parallel \to 0$, the Doppler shift in frequency is approximately obeyed. Consequently, regardless of the nature of the 2D layer represented in the dispersion equation we may replace $\omega \to \omega - \mathbf{q}_\parallel \cdot \mathbf{v}_d$ in the dispersion equation in the presence of an applied electric field at long wavelengths.

II. NUMERICAL RESULTS AND DISCUSSION

We shall treat the solution frequencies $\omega_\pm(q_\parallel)$ as complex variables with $\mathrm{Im}[\omega_\pm(q_\parallel)] \geq 0$, where $\mathrm{Im}[\omega_\pm(q_\parallel)] > 0$ implies finite growth rates $\gamma_\pm(q_\parallel) = \mathrm{Im}[\omega_\pm(q_\parallel)]$ for two split plasmon modes. Since $\epsilon(q_\parallel, \omega)$ is a complex function, we ask for $\mathrm{Re}[\epsilon(q_\parallel, \omega)] = \mathrm{Im}[\epsilon(q_\parallel, \omega)] = 0$. Therefore, we are left with damping-free plasmon modes in the spatial domain in the system but they still face possible instability in the time domain due to $\mathrm{Im}[\omega_\pm(q_\parallel)] > 0$.

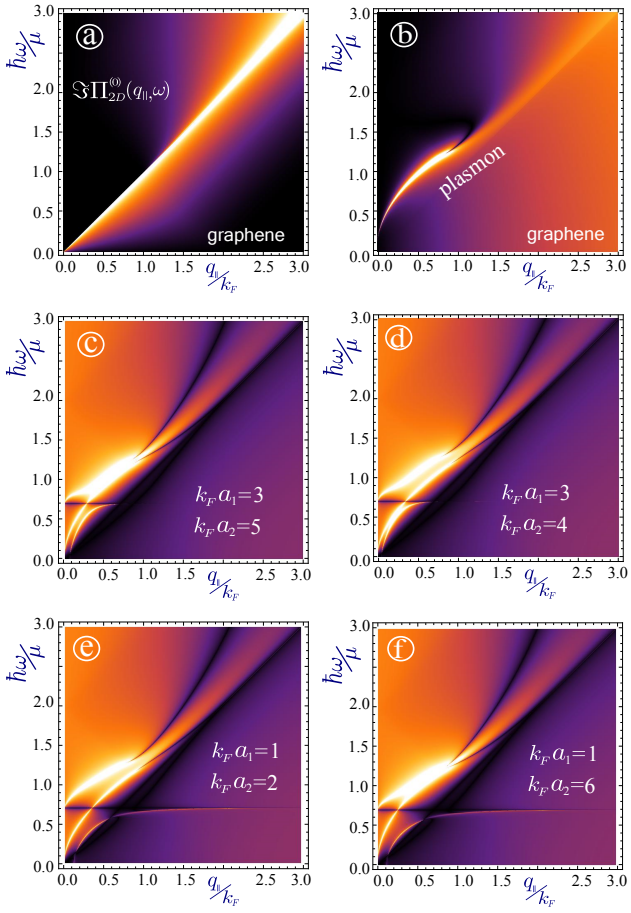

FIG. 3: (Color online) Particle-hole modes and plasmon dispersion for pristine graphene and for a hybrid system consisting of a heavily doped semiconductor interacting with two layers. Panel (a) presents the single-particle excitation spectrum, panel (b) shows the plasmon spectrum for a single layer of free standing graphene with no energy gap. Panels (c)-(f) show the plasmon excitations for various chosen distances between the surface and the layers, so that $k_F a_1 = 3$ and $k_F a_2 = 5$ are shown in panel (c), $k_F a_1 = 3$ and $k_F a_2 = 4$ in panel (d), $k_F a_1 = 1$ and $k_F a_2 = 6$ in panel (e). Also, $k_F a_1 = 1$ and $k_F a_2 = 6$ are chosen in panel (f).

The number of plasmon excitation branches for chosen $q_{\|}$ as well as the instability domain depends on the magnitude of the drift current and also on the distance between the constituents of the hybrid system. In Fig: 2, we show the complex plasma frequency solutions of our dispersion equation, with the real parts representing the dispersion, and the imaginary part corresponding to the rate of growth of the instability (inverse of $\Im\omega$). For a hybrid system made up of a semi-infinite heavily doped semiconductor and a 2D layer, we obtain two plasmon frequency solutions in the absence of a current. As the current is increased,

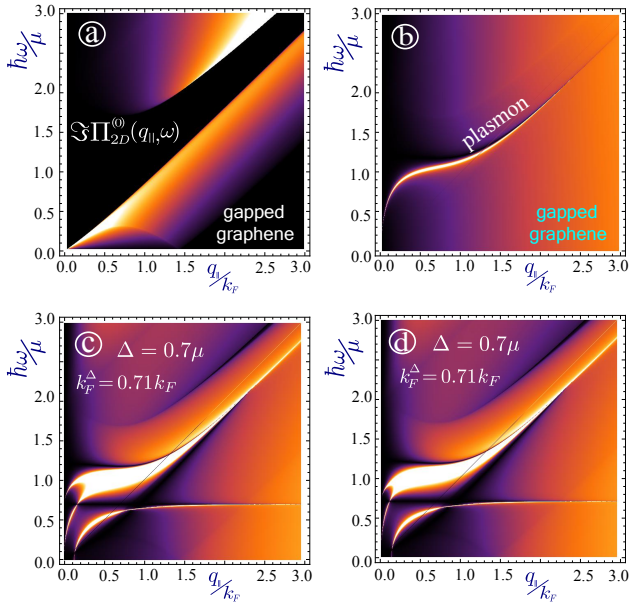

FIG. 4: (Color online) Particle-hole mode region and plasmon dispersion relation for free standing gapped graphene and for a hybrid system consisting of a heavily doped semiconducting substrate and two layers of gapped graphene with a large energy gap. In panel (a), we show the particle-hole continuum for gapped graphene. Panel (b) shows the plasmon dispersion for a single layer of gapped graphene. The energy gap is $\Delta = 0.7\mu$ for all the panels, so that the Fermi momentum is $k_F^{\Delta} = \sqrt{\mu^2 - \Delta^2}/(\hbar v_F) = 0.71 k_F^{\Delta=0}$. Panel (c) shows the case with $k_F a_1 = 3$ and $k_F a_2 = 5$ and in panel (d), we choose $k_F a_1 = 3$ and $k_F a_2 = 10$.

another solution with positive real part of the frequency may be determined, but there may be no imaginary part of this solution until the current reaches a critical value. The instability is closely connected to the observed closed loop of the real solution. Mathematically, it could be explained by the fact that for an even power equation with real coefficients for zero current all the solutions must be complex conjugated, e.g., have identical real parts.

We now turn to discuss the plasmon dispersion for a hybrid semi-infinite conductor and *two* layers of graphene, both with and without an energy gap. First, we investigate the single-particle excitation region responsible for Landau damping, outside of which undamped plasmons could be observed. The regions of the undamped plasmons is given by solving $\Im\Pi^0_{2D}(q_\parallel, \omega) = 0$. The results are presented in Fig. 3(a) for gapless grpahene, and in Figs. 4(a) and 5(a) for large (0.7μ) and small (0.2μ) energy band gap. Next, we show the plasmon in a single graphene layer for each case [13–15]. If there is no energy gap [see Fig. 3(b)] or its

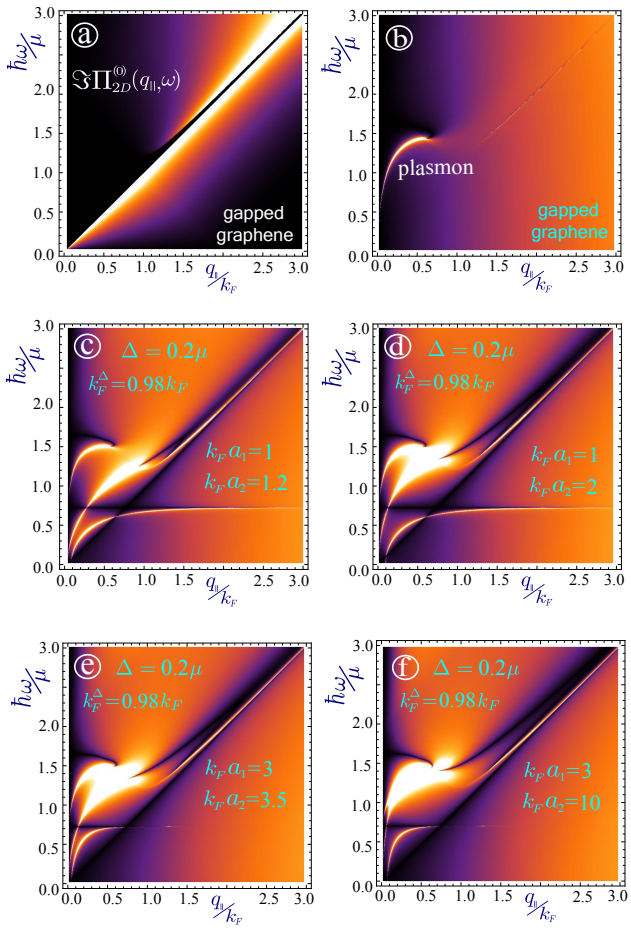

FIG. 5: (Color online) Density plots of the plasmon dispersion relations for a composite system of a semi-infinite heavily doped semiconductor and two graphene layers, with small energy gap. The energy gap is $\Delta = 0.2\,\mu$ for all the panels, so that the Fermi momentum is $k_F^{\Delta} = \sqrt{\mu^2 - \Delta^2}/(\hbar v_F) = 0.98 k_F^{\Delta=0}$. Panel (a) shows the single-particle excitations regions, panel (b) demonstrates the behavior of the plasmons for a single layer of free standing gapped graphene. All the other panels show the plasmon dispersion relation for the hybrid system. Panels (c) and (d) correspond the choice of $k_F a_1 = 1$ and $k_F a_2 = 1.2$ in (c) and $k_F a_1 = 1$ and $k_F a_2 = 2$ in (d). Panel (e) shows the case of $k_F a_1 = 3$ and $k_F a_2 = 3.5$, while in panel (f), we choose $k_F a_1 = 3$ and $k_F a_2 = 10$.

value is small (compared with the chosen gap) in Fig. 5(b), the plasmon is undamped only for a small range of $q_{\|}$. In contrast, for large energy gap, Fig. 4(b) shows that an undapmed plasma is found for a larger range of the wave vector.

Finally, we consider the plasmon dispersion when there are two 2D layers and a semi-infinite conductor with free carriers. Our solutions are determined by the location of the

particle-hole mode regions for each case, so that we obtain longer undamped plasmon branches for the case of gapped graphene, shown in Figs. [4](c) and (d). The distance between the surface and each of the 2D layers is also an important factor. When the larger distance a_2 is chosen, the middle plasmon branch, i.e., the one which starts from the origin with a bigger slope, tends to get close to coincide with the the uppermost branch, which starts from $\omega^{(0)} = \omega_p/\sqrt{2}$. For finite energy gap, the 'surface' plasmon mode shows much brighter and broader peak, compared to the lowest branch as depicted in Figs. 4(b)-4(d) and Figs. 5(c)-5(f).

III. CONCLUDING REMARKS

In summary, we are proposing a hybrid quantum plasmonic device which employs 2D layers in combination with a thick conducting material. We find that the spiler emits electromagnetic radiation when a current is passed through the 2D layer to make the plasmons become unstable at a specific frequency and wave number and grow over a period of time which is determined by the positive imaginary part of its complex frequency. It is possible to change the range of plasmon instability by selecting the properties of the nanosheet or frequency of the surface plasmon, i.e., the substrate. The surface plasmon plays a crucial role in giving rise to the Rabi-like splitting and the concomitant streams of quasiparticles whose phase velocities are in opposite directions when the instability takes place. The emitted electromagnetic radiation may be collected from regions on the surface that are convenient.

Promising sources of terahertz (THz) radiation have been investigated over the years. These frequencies cover the electromagnetic spectrum from microwave to infrared. Epitaxial growth of hybrid layers of semiconductors resulted in quantum well structures emitting high power THz across a wide frequency range. So far, only ultra-long wavelength emission has been reported. Our work shows how we may modify this limitation with the use of the proposed hybrid structure through a spontaneous generation of plasmon excitations and subsequent Cherenkov radiation at sufficiently high draft velocities.

Acknowledgments

This research was supported by contract # FA 9453-13-1-0291 of AFRL. DH would like to thank the Air Force Office of Scientific Research (AFOSR) for its support.

---

[1] U. Banin, Y. Ben-Shahar, and K. Vinokurov, Chem. Mater. **26**, 97 (2014).

[2] K. A. Brown, Q. Song, D. W. Mulder, and P. W. King, ACS Nano (2014) [DOI: 10.1021/nn504561v].

[3] P. S. Dilsaver, M. D. Reichert, B. L. Hallmark, M. J. Thompson, and J. Vela, J. Phys. Chem. C **118**, 21226 (2014).

[4] N. Liakakos, C. Gatel, T. Blon, T. Altantzis, S. Lentijo-Mozo, C. Garcia-Marcelot, L.-M. Lacroix, M. Respaud, S. Bals, G. Van Tendeloo, and K. Soulantica, Nano Lett. **14**, 2747 (2014).

[5] L. J. Hill, N. E. Richey, Y. Sung, P. T. Dirlam, J. J. Griebel, E. Lavoie-Higgins, I.-B. Shim, N. Pinna, M.-G. Willinger, W. Vogel, J. J. Benkoski, K. Char, and J. Pyun, ACS Nano **8**, 3272 (2014).

[6] X. Ye, D. R. Hickey, J. Fei, B. T. Diroll, T. Paik, J. Chen, and C. B. Murray, J. Am. Chem. Soc. **136**, 5106 (2014).

[7] S. Blumstengel, S. Sadofev, C. Xu, J. Puls, R. L. Johnson, H. Glowatzki, N. Koch, and F. Henneberger, Phys. Rev. B **77**, 085323 (2008).

[8] M. Fu, K. Wang, H. Long, G. Yang, P. Lu, F. Hetsch, A. S. Susha, and A. L. Rogach, Appl. Phys. Lett. **100**, 063117 (2012).

[9] J. A Kurzman, M.-S. Miao, and R. Seshadri, J. Phys.: Condens. Matt. **23**, 465501 (2011).

[10] G. Wang, X. Jiang, M. Zhao, Y. Ma, H. Fan, Q. Yang, L. Tong, and M. Xiao, Opt. Expr. **20**, 29472 (2012).

[11] G. Gumbs, A. Iurov, and D. H. Hunag, arXiv:1410.2851 [cond-mat.mtrl-sci] (2014).

[12] N. J. M. Horing, H. C. Tso, and G. Gumbs, Phys. Rev. B **36**, 1588 (1987).

[13] S. Das Sarma and A. Madhukar, Phys. Rev. B **23**, 805 (1981).

[14] B. Wunsch, T. Stauber, F. Sols, and F. Guinea, New J. Phys. **8**, 318 (2006).

[15] P. K. Pyatkovskiy, J. Phys.: Condens. Matt. **21**, 025506 (2009).